NANO LETTERS

2009
Vol. 9, No. 10
3603-3607

Sacrificial Ionic Bonds Need To Be Randomly Distributed To Provide Shear Deformability

Markus A. Hartmann[†,‡] and Peter Fratzl[*,‡]

Institute of Physics, University of Leoben, Franz-Josef Strasse 18, A-8700 Leoben, Austria, and Max-Planck-Institute of Colloids and Interfaces, Department of Biomaterials, Am Mühlenberg 1, D-14476 Potsdam, Germany

Received June 8, 2009; Revised Manuscript Received August 17, 2009

ABSTRACT

Multivalent ions are known to allow for reversible cross-linking in soft biological materials, providing stiffness and extensibility via sacrificial bonds. We present a simple model where stiff nanoscale elements carrying negative charges are coupled in shear by divalent mobile cations in aqueous media. Such a shear coupling through a soft glue has, indeed, been proposed to operate in biological nanocomposites. While the coupling is elastic and brittle when the negative charges are periodically arranged, sufficient randomness in their distribution allows for large irreversible deformation.

Dependent on their function, biological as well as technical materials have to possess different, often contradictory, properties. In load-bearing materials, such as bone, a high stiffness has to be reconciled with an elevated toughness. A high stiffness, defined as the initial slope of the stress−strain curve, means that the material deforms only little with applied load. On the other hand, toughness is a measure of how much energy has to be put into the material to break it. In one-component materials, stiffness and toughness are typically contradictory properties. A strategy often followed by nature to build materials that are both stiff and tough is to construct hierarchically organized composite materials from two or more constituents that possess one of the desired properties.[1] In bone collagen, a soft, but tough protein, and hydroxyapatite, a stiff, but brittle mineral, are arranged in such a way, that the composite bone shows a toughness comparable to that of collagen and a stiffness close to the one of hydroxyapatite.[2] This is achieved by the staggered arrangement of mineral particles which distribute tensile loads such that the mineral particles are predominantly loaded in tension, while the soft matrix transmits the loads via shear.[3] In the framework of this model, bone achieves its elevated stiffness by the large aspect ratio of mineral particles, despite the small stiffness of the matrix phase. On the other hand the toughness of bone can be considerable enhanced by the shape of the stress−strain curve of the soft matrix in shear. If the maximum shear stress in the matrix can be kept below a certain value (dependent on the fracture stress and the aspect ratio of the mineral particles), failure of the brittle mineral particles can be prevented.[1] Thus, understanding the shear behavior of the matrix is of great importance to understand the mechanical behavior of bone as a whole.

Recent experiments using atomic force microscopy show evidence that the behavior of the soft matrix is governed by electrostatic interactions, most probably between negatively charged proteins and divalent Ca ions.[4,5] Other experiments measuring the strain rate and temperature dependence of the plastic deformation in bone found that the activation energy of the basic step of plastic deformation is approximately 1.1eV and the corresponding activation volume 0.6 nm^3.[6] These values are much too high to be associated with the breaking of hydrogen bonds, as well as much too low to be associated with the breaking of covalent bonds. On the other hand, electrostatic bonds mediated by divalent ions are in the correct order of magnitude. These bonds are called sacrificial, since, first, they are much weaker than the bonds holding the structure together. Second, they can form and open reversibly, and third, they dissipate a large amount of energy, before the structural bonds collapse.[4] Sacrificial bonds based on multivalent cations cross-linking negatively charged molecules have also been reported in a range of other materials from seashells[7] to mussel fibers.[8,9]

Motivated by these observations we present a model to describe the shear behavior of the soft matrix of biological materials which is solely governed by electrostatics (see Figure 1). Our model consists of two negatively charged, parallel plates representing extrafibrillar mineral particles or other stiff components in the nanocomposite. The negative charges, which were assumed pointlike and condensed on

* Corresponding author, Peter.Fratzl@mpikg.mpg.de.
† University of Leoben.
‡ Max-Planck-Institute of Colloids and Interfaces.

10.1021/nl901816s CCC: $40.75
Published on Web 08/31/2009

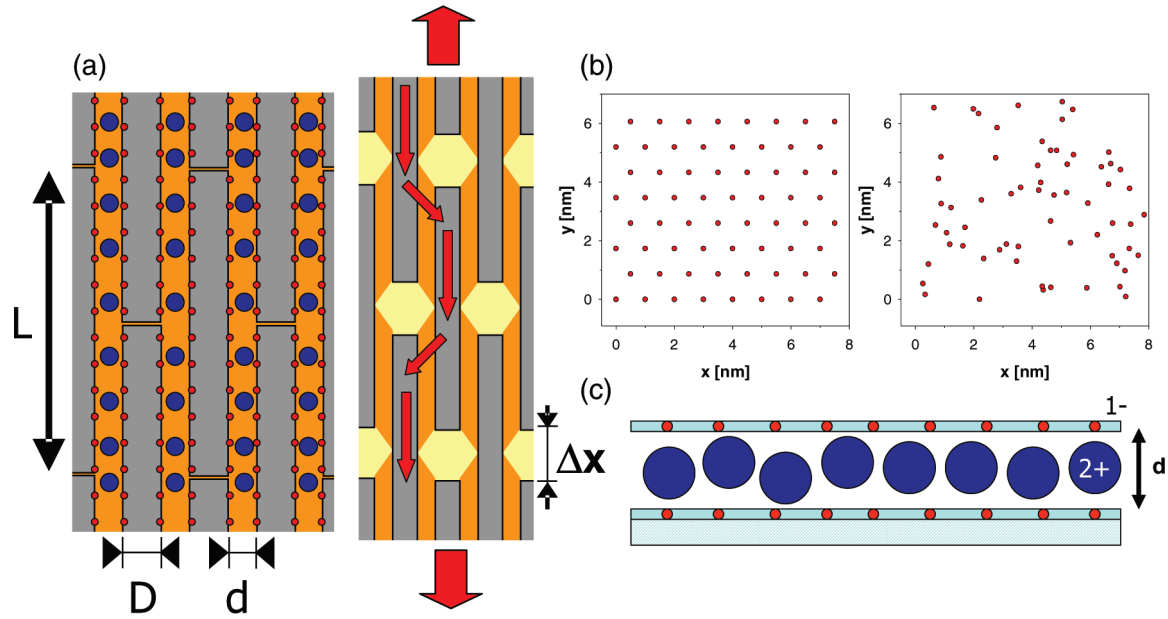

Figure 1. A schematic sketch of the system investigated in this Letter. (a) Unloaded and loaded mineralized collagen fibrils. The mineral particles—arranged in a staggered manner—are depicted in gray, while orange areas represent the soft matrix. Negative charges are shown in red; while blue circles denote the positively charged counterions. When the system is loaded in tension, the mineral particles are loaded in tension and the matrix transmits the load via shear, as is indicated by the red arrows (figure adapted from ref [1]). (b) Top view of the charge distribution on the bottom plate in the model system: ordered configuration (left) and (one of the) random configurations (right). (c) Side view of the system. Negative charges are depicted in red, while counterions are shown in blue.

the two plates, stand for negatively charged, noncollagenous proteins, which are anchored to the mineral phase, e.g., phosphorylated osteopontin.[10] Assuming a nonhomogeneous charge distribution is crucial for our model, since homogeneously charged walls do not show any resistance against shear due to symmetry. A similar model describing sliding friction between two charged plates was introduced in ref 11. In our model the bottom plate was held fixed, while the top plate could move in x, y, and z directions. Applying an external force F_{ext} on the upper plate in the x direction and measuring the corresponding displacement yields force−displacement curves corresponding to shear. Two extreme conditions for the charge distribution on the two plates were investigated. First, the negative charges were set according to a regular, triangular lattice, and second, the charges were placed randomly (see Figure 1b). In both scenarios the same average charge density was used. Overall charge neutrality was ensured by divalent positively charged counterions, which could move freely between the two plates (see Figure 1c). In the present Letter we restrict ourselves to the salt-free case; i.e., only counterions were present. The counterions were modeled as charged hard spheres with a hard core radius $R = 0.11$ nm and charge $Z = 2$. Thus, the interaction energy E of two charges is Coulombic and given by

$$E(r_{ij})/k_BT = \begin{cases} L_B \dfrac{Z_i Z_j}{r_{ij}} & r_{ij} \geq R_i + R_j \\ \infty & r_{ij} < R_i + R_j \end{cases} \quad (1)$$

where r_{ij} is the distance between charges i and j, Z_i and Z_j are their corresponding charges, R_i and R_j are their radii ($R = 0$ for the negative charges,) and L_B the Bjerrum length, which has a value of ≈ 0.72 nm in aqueous solution at room temperature and gives the distance where the interaction of two unit charges equals thermal energy. The exact value of the Bjerrum length depends on the permittivity of the solvent, which is unknown for such a complicated situation as we find in, e.g., bone. Nevertheless, the Bjerrum length is a multiplicative constant, which only rescales the energy or temperature scale, respectively. Thus, even if the exact value of the Bjerrum length is not known, the results presented remain valid. k_B is Boltzmann's constant and T the temperature. Monte Carlo simulations were carried out in the (NPT) ensemble with 192 charges present in the system (128 negative charges and 64 counterions). For each applied load 1000 configurations separated by 10000 Monte Carlo steps (1 Monte Carlo step corresponds to one jump trial per charge) were obtained, which were then used to calculate the mean displacement in the x direction. In x and y directions periodic boundary conditions were used, while hard wall boundary conditions—imposed by the two plates—were used in the z direction. For the energy calculation the minimum image convention was applied. Furthermore, the two walls were assumed to have the same dielectric constant as the solvent; i.e., no electrostatic images were taken into account. For each of the two different charge distributions (regular and random, respectively) simulations were performed with two different (average) charge densities, corresponding to the charge density of a triangular lattice with one charge per lattice point and lattice constants 1 and 0.5 nm, respectively.

In all cases the system showed an effective attraction between the likewise charged plates in accordance with results from the strong-coupling theory for the electrostatics of homogeneously[12−14] and disordered charged walls.[15,16] This

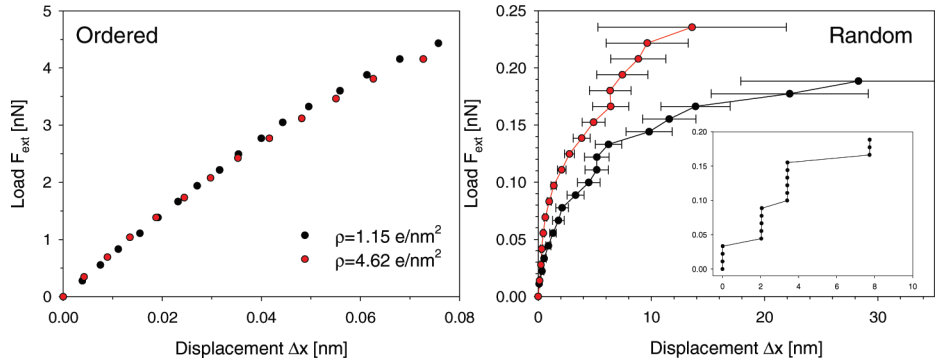

Figure 2. Averaged load−displacement curves for the investigated systems for two different charge densities ρ: left, for the case of the regular lattice; right, for the disordered case. Error bars denote the standard deviation of the mean obtained from up to 25 independent simulation runs. The inset shows a typical load−displacement curve for a single simulation run. A pronounced stick−slip mechanism responsible for the plastic behavior of the material can be observed.

effective attraction made the plates collapse; an average thickness of the system of $d \approx 0.25$ nm was found. The equilibrium thickness slightly decreased for higher charge density and for the ordered state compared to the random state. In Figure 2 the load−displacement curves for the two different charge densities ($\rho = 1.15$ and 4.62 e/nm^2, respectively) and for the ordered and the random case are shown. The latter curve was obtained by averaging 25 independent simulation runs. The shown error bars correspond to the standard deviation of the mean. The large error bars for large loads stem from the fact that—since the configuration is random—different simulation runs can bear different maximum loads. Thus, the higher the load, the fewer the simulation runs that were able to sustain this load, leading to a fewer number of data points for averaging. Figure 2 shows that the arrangement of charges (ordered and nonordered) has a tremendous effect on the mechanical behavior of the system. In the case of the ordered system (Figure 2, left) the maximum load the system can bear is approximately 4.2 nN, which reduces to only 0.2 ± 0.05 and 0.22 ± 0.08 nN in the case of the nonordered system for the low and high charge density, respectively (Figure 2, right). One should bear in mind that the maximum load a system can withstand is an extensive variable; i.e., it scales with the system size. Thus, if values of the maximum load for different system sizes are compared, load divided by area, i.e., the stress, is the adequate variable to work with. The experienced maximum displacements of the two systems show the opposite behavior; it is only ≈0.08 nm for the ordered system, while it is 39 ± 12 nm and 21 ± 8 nm, respectively, for the disordered system, which makes a difference of a factor 250−500. Accordingly the dissipated energy until failure of the material, i.e., the area under the load−displacement curve, is $\approx 45\ k_BT$ in the case of the regular lattice (for both charge densities) and $1170 \pm 280\ k_BT$ and $780 \pm 320\ k_BT$ for the two random configurations, respectively.

In the case of the ordered arrangement, the plates move until the negative charges exactly match and one ion forms a Coulombic bridge between them. In this case the load−displacement curves reflect the electrostatic potential of such a configuration, which shows nonlinear, but elastic, behavior for large deformations. Interestingly the curves coincide for the two investigated charge densities, which shows that the system can be understood as the parallel coupling of independent bonds. Consequently the mechanical properties like shear modulus and strength, which are—in contrast to the maximum load the system can bear—independent of the system size, scale linear with the charge density ρ. All bonds are loaded in exactly the same way and fail collectively when the strength of the system is exceeded (see also top row of supplemental Figure 4 in Supporting Information). Thus, the material behavior can be described as nonlinear elastic and brittle.

In the case of a random arrangement, the situation changes. Most strikingly the curves do not coincide for the two investigated charge densities. Thus, the situation can no longer be described by isolated bonds. Higher charge densities lead to a stiffness higher as would be expected from the trivial, linear scaling with charge density. While the maximum load is comparable for both densities, the maximum displacement is different, i.e., lower for the higher charge density. The mechanical behavior of the system can be understood by a stick−slip mechanism: The inset in Figure 2 shows a typical load−displacement curve of a single run. At initially small loads the system deforms elastically until the load reaches a critical value and the material starts slipping. But since the system is unordered, after some slipping it eventually finds a new, more stable configuration that withstands further elongation (see bottom row of supplemental Figure 4 in Supporting Information). After completion of such a slipping event, the displacement will not go back to zero, when the load is released. Thus, the material has undergone permanent deformation by shearing of the interface. The lower maximum displacement for higher charge densities can be explained by the fact that, the lower the charge density, the larger the mean distance between clusters of charge that can withstand further elongation. Thus, the system has to flow a larger distance to find a new, stable configuration.

It is interesting to estimate the mechanical properties of a composite material as sketched in Figure 1a, which resembles a multilayer system. Electrostatic coupling of constituents of other geometric forms, e.g., fibers, will not considerably

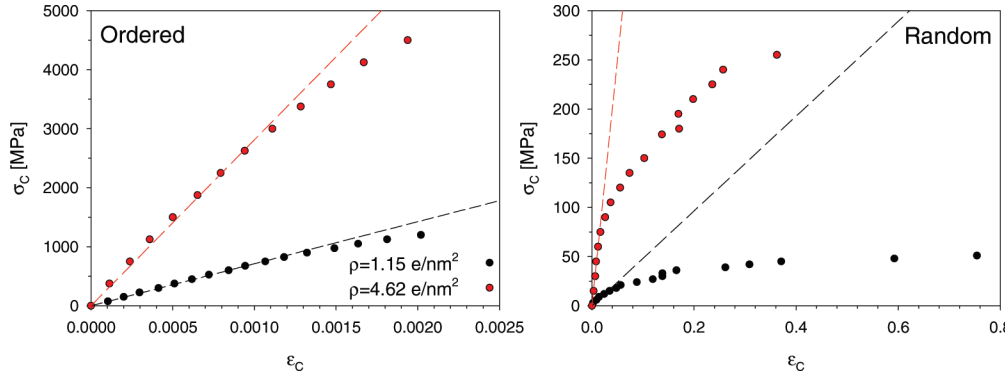

Figure 3. The stress−strain curves for the composite material. Left for the ordered case, and, right, for the random arrangement. Dashed lines show a linear fit of the first, linear, part of the curves yielding the elastic modulus of the composite.

change the results, as long as it is ensured that additional geometric constraints, like geometric blocking due to, e.g., the curvature of fibers, can be prevented. For simplicity let the composite under consideration be composed of an inextensible, staggered phase and the matrix as modeled in this Letter. Thus, we neglect the elastic modulus of the matrix, as well as any constituents other than the counterions. Following ref 1 we find

$$\sigma^{\mathrm{C}} = \frac{D+d}{D}\sigma^{\mathrm{P}} \tag{2}$$

$$\varepsilon^{\mathrm{C}} = \frac{2\Delta x}{\rho D} \tag{3}$$

$$\tau^{\mathrm{M}} = \frac{2}{\rho}\sigma^{\mathrm{P}} \tag{4}$$

where the superscripts denote the composite, the particle, and matrix phase, respectively. $D = 2.5$ nm and $d \ll D$ denote the thickness of the particles and of the glue layer, respectively. $\rho = 30$ is the aspect ratio of the particles[17] and Δx the displacement of the matrix for a given load (see also Figure 1a for an explanation of the parameters). In Figure 3 the resulting stress−strain curves for the composite are shown. Fitting the first points of the curve with a linear regression gives the elastic modulus for the composite. We find unrealistically high values $E \approx 700$ and $E \approx 2800$ GPa for the case of the regular charge distribution and the low and high charge density, respectively (which reflects the linear scaling of the elastic parameters with the charge density). For the case of the random configuration, we correspondingly find $E \approx 0.5$ and $E \approx 5$ GPa. Integration of the stress−strain curves yields the energy necessary to break the material, which can be interpreted as an indication for the toughness of a material. While the area under the stress−strain curve is 1.4 and 5 MJ/m^3 for the ordered case, it is 46 and 275 MJ/m^3 for the random arrangement, respectively. Measured elastic moduli of bone typically range from 10 to 20 GPa,[18] which is remarkably close to the value of 5 GPa that we find in our simple model for $\rho = 4.62$ e/nm^2 and a random arrangement of charges. Keeping in mind that we were investigating the two extreme conditions of the arrangement of charges, totally ordered and completely random, respectively, we have shown that by changing only the arrangement of charges, not their concentration, a change in the elastic modulus of the composite of more than 3 orders of magnitude can be achieved, while the toughness of the composite changes simultaneously by a factor of 50.

While the model presented in this Letter was motivated mainly by the experimental findings concerning the soft matrix in bone, it is far more general. The combination of a soft matrix experiencing shear and stiff inclusions loaded in tension or compression is a common design principle of many natural materials. While the situation sketched in Figure 1a aims at describing the situation in bone, a stick−slip mechanism has also been proposed to account for the observed load−displacement curves in wood, where the stiff inclusions are cellulose fibrils, embedded in a soft matrix of hemicellulose and lignin.[19] To keep the model as simple as possible, several simplifications were made. The negative charges were assumed pointlike and condensed on the mineral platelets. In reality negative charges are provided by proteins anchored to the mineral, which carry several charges at once.[20] Including a more realistic description of this scenario will also add some more stiffness to the matrix, due to, e.g., steric hindrance of the different proteins. Furthermore, the stiffness of the protein backbone can have significant effects on the mechanical performance of the system. The effect of the elasticity of the protein backbone on the rupture strength of protein domains stabilized by hydrogen bonds was investigated in ref 21. There it was shown that due to entropic elasticity of the backbone only small clusters of hydrogen bonds can simultaneously contribute to the rupture process, leading to a critical maximal length of strand lengths in β-sheets. For the present these effects are neglected in our model, but their investigation in a more refined model seems promising. Another simplification we made is to study the counterion only case, whereas in physiological solution a large amount of additional salt is present. The future investigation of the effect of added salt will provide important information, since there are indications that by changing external parameters like salt concentration or pH value one can considerably alter the mechanical performance of bone.[22] The presented model gives a framework to describe such effects and provides a molecular

description of the important interface between mineral and matrix in biological materials.

Supporting Information Available: Illustration of different deformation behavior in the case of ordered and disorded configurations. This material is available free of charge via the Internet at http://pubs.acs.org.

References

(1) Fratzl, P.; Weinkamer, R. *Prog. Mater. Sci.* **2007**, *52*, 1263.
(2) Fratzl, P.; Gupta, H. S.; Paschalis, E. P.; Roschger, P. *J. Mater. Chem.* **2004**, *14*, 2115.
(3) Jäger, J.; Fratzl, P. *Biophys. J.* **2000**, *79*, 1737.
(4) Fantner, G. E.; Hassenkam, T.; Kindt, J. H.; Weaver, J. C.; Birkedal, H.; Pechenik, L.; Cutroni, J. A.; Cidade, G. A. G.; Stucky, G. D.; Morse, D. E.; Hansma, P. K. *Nat. Mater.* **2005**, *4*, 612.
(5) Fantner, G. E.; Adams, J.; Turner, P.; Thurner, P. J.; Fisher, L. W.; Hansma, P. K. *Nano Lett.* **2007**, *7*, 2491.
(6) Gupta, H. S.; Fratzl, P.; Kerschnitzki, M.; Benecke, G.; Wagermaier, W.; Kirchner, H. O. K. *J. R. Soc., Interface* **2007**, *4*, 277.
(7) Smith, B. L.; Schäffer, T. E.; Viani, M.; Thompson, J. B.; Frederick, N. A.; Kindt, J.; Belcher, A.; Stucky, G. D.; Morse, D. E.; Hansma, P. K. *Nature* **1999**, *399*, 761.
(8) Holten-Andersen, N.; Fantner, G. E.; Hohlbauch, S.; Waite, J. H.; Zok, F. W. *Nat. Mater.* **2007**, *6*, 669.
(9) Holten-Andersen, N.; Mates, T. E.; Toprak, M. S.; Stucky, G. D.; Zok, F. W.; Waite, J. H. *Langmuir* **2009**, *25*, 3323.
(10) Gericke, A.; Qin, C.; Spevak, L.; Fujimoto, Y.; Butler, W. T.; Sorensen, E. S.; Boskey, A. L. *Calcif. Tissue Int.* **2005**, *77*, 45.
(11) Herminghaus, S. *Phys. Rev. Lett.* **2005**, *95*, 264301.
(12) Netz, R. R. *Eur. Phys. J. E* **2001**, *5*, 557.
(13) Moreira, A. G.; Netz, R. R. *Phys. Rev. Lett.* **2001**, *87*, 078301.
(14) Guldbrand, L.; Jönsson, B.; Wennerström, H.; Linse, P. *J. Chem. Phys.* **1984**, *80*, 2221.
(15) Fleck, C. C.; Netz, R. R. *Europhys. Lett.* **2005**, *70*, 341.
(16) Naji, A.; Podgornik, R. *Phys. Rev. E* **2005**, *72*, 041402.
(17) Weiner, S.; Wagner, H. D. *Annu. Rev. Mater. Sci.* **1998**, *28*, 271.
(18) Currey, J. D. *Bones: structure and mechanics*; Princeton University Press: Princeton, NJ, 2002.
(19) Keckes, J.; Burgert, I.; Frühmann, K.; Müller, M.; Kölln, K.; Hamilton, M.; Burghammer, M.; Roth, S. V.; Stanzl-Tschegg, S.; Fratzl, P. *Nat. Mater.* **2003**, *2*, 810.
(20) Salih, E.; Ashkar, S.; Gerstenfeld, L. C.; Glimcher, M. J. *J. Biol. Chem.* **1997**, *272*, 13966.
(21) Keten, S.; Buehler, M. J. *Nano Lett.* **2008**, *8*, 743.
(22) Kotha, S. P.; Walsh, W. R.; Pan, Y.; Guzelsu, N. *Bio-Med. Mater. Eng.* **1998**, *8*, 321.

NL901816S